Level set simulation of directed self-assembly during epitaxial growth

X. Niu,[1] R. Vardavas,[2] R. E. Caflisch,[1,2] and C. Ratsch[2,*]
[1]*Department of Material Sciences and Engineering, University of California, Los Angeles, Los Angeles, California 90095, USA*
[2]*Department of Mathematics, University of California, Los Angeles, Los Angeles, California 90095, USA*
(Received 31 August 2006; published 2 November 2006)

We study the effect of a spatially varying potential energy surface on the self-organization of nanoscale patterns during epitaxial growth. The computational approach is based on the level set method. Our results have an implication for guided self-assembly of nano patterns, which is a promising new technique for many technological applications. Both kinetic as well as thermodynamic effects can lead to ordering, and we discuss the competition between these two effects.

DOI: 10.1103/PhysRevB.74.193403 PACS number(s): 68.43.Hn, 68.55.Ac, 68.65.Hb, 68.65.La

Highly ordered and uniformly sized nano patterns play an increasingly important role for many technological applications. So-called quantum dots for semiconductor systems open the door to new opto-electronic devices. Ordered nano patterns in metallic systems can be used for storage devices[1] or nanocatalysis.[2] Critical factors for the performance of all such devices are that the patterns are all within a certain size range (which depends on the material) and that the dots are all equal in size. A common approach to synthesizing nano patterns is through vacuum deposition techniques, where the desired structures grow epitaxially on a substrate. It is therefore the focus of a large number of studies to understand the formation and growth of nano patterns[3] and to control their formation and size distribution.

There are various approaches to obtaining arrays of equally sized and spaced nano patterns. One way is often referred to as top-down, where islands nucleate in previously fabricated nucleation sites. But structures as small as a few nm are difficult to obtain with standard lithographic techniques. On the other hand, it has been observed for semiconductor systems that kinetic and/or thermodynamic factors spontaneously lead to the formation of quantum dots.[4–6] Moreover, under the right conditions, these quantum dots can be ordered laterally[7] or vertically.[8,9] This approach is often referred to as a bottom-up approach.

Guided or directed self-assembly is somewhere in-between. In this very promising approach, one still exploits kinetic or thermodynamic effects. However, it is the goal to control these effects by manipulating some conditions during the epitaxial growth process. Introduction of subsurface dislocation arrays have been suggested to be useful for this.[10,11] These buried dislocations introduce a long-range strain field, which alters the potential energy surface (PES). Similarly, islands that are capped by a buffer layer of a different material introduce a long-range strain field. It has been shown by density-functional theory (DFT) calculations for metal systems[12] and semiconductor systems[13] that both the adsorption energy E_{ad} and the transition energy E_{trans} of the PES change upon strain.

In this Brief Report, we discuss simulations that demonstrate that a properly modified PES for adatom diffusion can lead to self-organization of nano patterns. Adatom diffusion is described by a rate for surface diffusion, which is $D=D_0\exp(-\Delta E/k_BT)$, where D_0 is a prefactor (chosen to be 10^{13} s^{-1}), k_B is the Boltzman constant, T is the temperature, and ΔE is the energy barrier for surface diffusion, given by $\Delta E=E_{\mathrm{trans}}-E_{\mathrm{ad}}$. Most previous work on directed self-assembly of regular nano patterns has only focused on thermodynamic arguments, where only variations of E_{ad} are considered.[14–16] Some studies have also included kinetic arguments where also E_{trans} is varied.[17–19] But this was typically done in a single parametrization. Here, we treat E_{ad} and E_{trans} as independent parameters and study growth systematically as a function of them. We show that self-organization can be obtained by a modification of E_{trans} (kinetic limit), as well as a modification of E_{ad} (thermodynamic limit). The PES of a real system will typically be in-between, and we will discuss the competition between the two limits, where the two possible variations are either in phase, or out of phase. A main conclusion of our work is that it is not only thermodynamics that lead to directed self-assembly, but that, in fact, kinetic effects are equally important. We therefore assert that future work on guided self-assembly should consider kinetics and thermodynamics.

We model epitaxial growth on a surface with a spatially varying, anisotropic PES using the level set (LS) approach to epitaxial phenomena.[20,21] We use dimensionless units for length, so that the lattice constant is $a=1$. In our implementation of the LS method, islands are resolved as atomistic in height but continuous in the lateral dimensions. The boundaries of islands of height $k+1$ are represented by the set of points $\mathbf{x}$ where a level set function $\varphi(\mathbf{x},t)=k$. Adatoms are represented by an adatom density $\rho(\mathbf{x},t)$, which is updated by solving the following diffusion equation:

$$\frac{\partial\rho}{\partial t}=F+\nabla\cdot(\mathbf{D}\,\nabla\,\rho)-2\frac{dN}{dt}+\nabla\cdot\left(\frac{\rho}{k_BT}\mathbf{D}(\nabla E_{\mathrm{ad}})\right). \quad (1)$$

In Eq. (1), $\mathbf{D}$ is a diffusion tensor where the diagonal entries are labeled $D_i(\mathbf{x})$ and $D_j(\mathbf{x})$, and correspond to diffusion along the two directions i and j. For simplicity, no other direction for diffusion is included (but could easily be incorporated). F is the deposition flux, dN/dt is the nucleation rate, and the last term is the thermodynamic drift, where k_B is the Boltzman constant and T is the temperature. We enforce a boundary condition $\rho(\mathbf{x})=\rho_{\mathrm{eq}}(D_{\mathrm{det}}(\mathbf{x}),\mathbf{x})$, where $D_{\mathrm{det}}(\mathbf{x})$ is a (spatially varying) detachment rate.[22] The nucleation rate is given by[21]

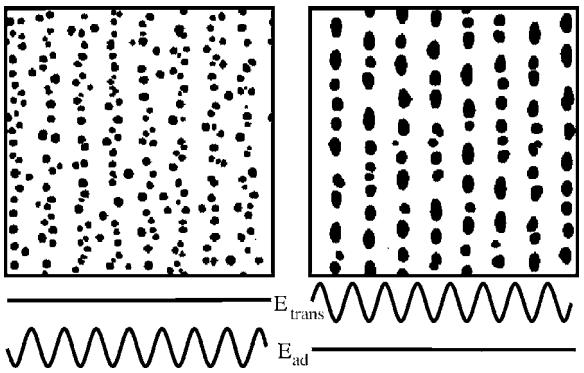

FIG. 1. Shown are the morphologies as obtained in the kinetic limit (right) and the thermodynamic limit (left) (top panels). A schematic of the envelope of the underlying variations of the PES is shown at the bottom for each case. Note that each period of the sinusoidal variation corresponds to 50 lattice constants.

$$dN/dt = \sigma_1 \langle [(D_i(\mathbf{x}) + D_j(\mathbf{x}))/2] \rho^2(\mathbf{x}) \rangle, \tag{2}$$

where σ_1 is the so-called capture number,[23] and the average $\langle\ \rangle$ is taken over all lattice sites.

The level set function φ evolves according to

$$\frac{\partial \varphi}{\partial t} + v_n |\nabla \varphi| = 0. \tag{3}$$

The normal velocity v_n is computed as

$$v_n = [\mathbf{n} \cdot \mathbf{D}(\nabla \rho)^- - \mathbf{n} \cdot \mathbf{D}(\nabla \rho)^+], \tag{4}$$

where $\mathbf{n}$ the island boundary normal, and the two terms correspond to diffusion of adatoms toward the island edge from the terraces above (+) and below (−) the island edge.

We assume a simple sinusoidal variation of E_{ad} and E_{trans}. More precisely, for the results shown in Fig. 1, we assume that the diffusion constant varies between $D=10^5$ s^{-1} and $D=10^7$ s^{-1} along the i direction, and that in fact $\log_{10} D$ varies sinusoidally. Diffusion is isotropic but spatially varying, and we use the notation $D=D_i(\mathbf{x})=D_j(\mathbf{x})$. A schematic of the variations of the PES is shown in the bottom panels of Fig. 1. The periodicity of the variation of the PES in the i direction was chosen to be 50 atomic spacings. This distance compares very well to the spacing between islands for stacked InAs islands on GaAs, which is about 50 nm,[8,9] or the spacing between reconstruction lines for the observed Herringbone reconstruction of Au/Au(111),[24] which is about 22.5 atomic spacings. We note that our approach can be used for any (complicated) PES. Although it may be difficult to obtain the proper PES for a specific system, we expect that different shapes of the PES would lead to qualitatively similar results (see also below). For example, the PES will vary more abruptly in the presence of defects or other features (such as steps or islands) near the surface, and will vary more smoothly if the strain-induced variation is due to buried defects[10,11] or islands.[8,9] In fact, we suggest that the depth of the defects (or the thickness of a buffer layer) is a parameter that can be varied in the experiment. We also use a simplified spatial variation of D_{det}, and vary it between 422 and 750 s^{-1}. Smaller or larger numbers for D_{det}, or even a constant D_{det} in the same range, lead to very similar results.

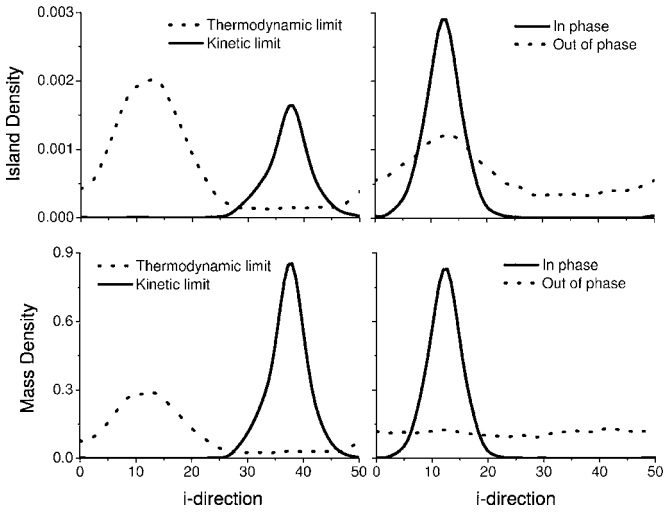

FIG. 2. The spatial variation of the island densities (top panels) and mass densities (bottom panels) for the two different PES shown in Fig. 1 (left panels) and Fig. 3 (right panels). Data were obtained as an average of at least 30 runs on a lattice of size 400×400.

The results shown in Fig. 1 correspond to the thermodynamic limit (left panel), where only E_{ad} is varied, and the kinetic limit (right panel), where only E_{trans} is varied. For the particular choices presented here, the spatial variation of the diffusion constant D is identical in both cases. The PES is varied only along the i direction, and is constant along the j direction. It is immediately evident from the morphologies that islands almost exclusively form along stripes in either limit. But in the kinetic limit, the islands are rather large, while they are much smaller in the thermodynamic limit. Closer inspection shows that the positions of most islands are inverted. This can also be seen in the left panels of Fig. 2, where we show the island densities (top) and mass densities (bottom) as a function of the i direction. Because of the periodicity of the PES, only 1/8 of the extent along the i direction is shown (i.e., from 0 to 50). Comparison of Fig. 1 and Fig. 2 reveals that in fact the islands nucleate in the region of fast diffusion (low potential energy barrier) in the kinetic limit, but nucleate in the region of slow diffusion in the thermodynamic limit, and that correspondingly all the mass is in these regions.

The explanation for this is the following: In the nucleation rate dN/dt in Eq. (2), the parameter σ_1 is essentially constant, so that dN/dt increases either when D increases, or when $\rho(\mathbf{x})$ increases. In the kinetic limit (without a thermodynamic drift), $\rho(\mathbf{x})$ is spatially constant (at least before islands start acting as sinks on the surface, which is the case in the nucleation phase), so that the nucleation rate is dominant in regions where D is large. We believe that this is also the limit that has been discussed in Ref. 17. However, once a thermodynamic drift is present, the adatom concentration is not constant, and is in fact largest in regions where E_{ad} has its minimum. If the drift term is large enough, dN/dt is dominated by a large ρ, which is in regions where D is small (large barrier). This is the limit that has also been discussed in a recent study by Yang *et al.*[15]

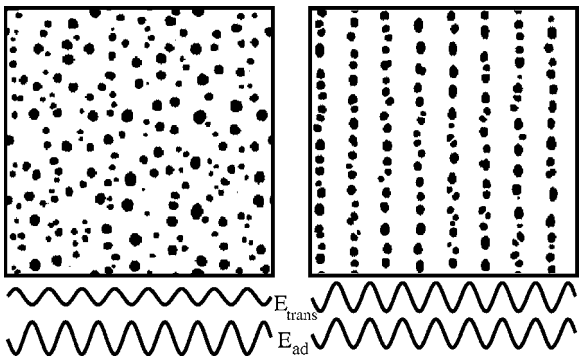

FIG. 3. Morphologies as obtained with out-of-phase (left) and in-phase (right) variations of E_{ad} and E_{trans}. A schematic of the envelope of the underlying variations of the PES is shown at the bottom for each case. Note that each period of the sinusoidal variation corresponds to 50 lattice constants.

We can now also understand why the islands are much larger in the kinetic limit: Here, nucleation is determined by a large diffusion constant. But the diffusion constant D also determines a characteristic length $l_{char} \sim D^{\chi}$, which characterizes the size of and spacing between islands. The positive exponent χ depends on the degree of reversibility (i.e., D_{det} and F).[25] This means that in regions of large D, islands are on average larger and fewer. On the other hand, in the thermodynamic limit, islands nucleate in the region of small D, where l_{char} is smaller, and hence there are more and smaller islands. This size variation for the island sizes has also been seen in the work of Mattsson and Metiu.[18] However, these authors did not observe the same ordering as discussed in our study because they considered a system where during growth the periodicity of the variation of the PED was much larger than l_{char}.

For systems where strain drives the variation of the PES, we expect that E_{ad} and E_{trans} vary at the same time. There are two possibilities: either, the variations of E_{ad} and E_{trans} are out of phase (i.e., E_{ad} increases when E_{trans} decreases, and vice versa), or they are in phase. We believe that both of these cases are physically realistic. For systems where a simple hopping mechanism is the dominant mechanism for diffusion, we expect an in-phase variation.[12,13] On the other hand, when diffusion is dominated by the concerted motion of several atoms (such as the exchange mechanism), or when more complicated reconstructions are present on the surface, out-of-phase variations are plausible.

Results for both of these cases are presented in Fig. 3. We show a schematic of the PES (bottom panels) and typical surface morphologies (top panels). The simulation parameters were chosen such that in the case of out of phase variations, the spatial variation of D is the same as in the results in Fig. 1. In the case of in-phase variations, we assume that E_{ad} and E_{trans} have the same variation, so that the diffusion constant is essentially spatially constant[26] with $D=10^6$ everywhere, and the envelope of the PES varies by 0.278 eV. In this case, the only effect that might lead to spatial inhomogeneities of island nucleation is the thermodynamic drift. Clearly, in the latter case, islands again all nucleate in the regions where the adsorption energy has its minimum. This is also evident from the island distribution and mass distribution shown in the right panels of Fig. 2. As explained above, nucleation is completely dominated by the larger value of ρ. One might refer to this situation as the true thermodynamic limit, as there is no competition between kinetic effects (spatially varying D) and the thermodynamic drift. On the other hand, when the variations of E_{ad} and E_{trans} are out of phase, preferred nucleation due to fast diffusion, and due to a thermodynamic drift, compete with each other in the different regions and very little spatial ordering is seen. In fact, in this case, the mass distribution is almost uniform as a function of i, while there are many more islands in the region of slow diffusion than in the region of fast diffusion (cf. Fig. 2).

The numbers chosen in our studies for the PES are simple model parameters, but are quite realistic numbers. For example, Brune *et al.* studied growth of Ag on Pt(111),[27] where the lattice mismatch is 4%. If Ag/Ag(111) is compressed by 4%, the energy barrier is lowered by approximately 30 meV,[12,27] which at $T=100$ K corresponds to a change of D of two orders of magnitude. For semiconductor systems the situation is more complicated, as these systems reconstruct on the surface, and the surface reconstruction changes upon small strains.[28] Nevertheless, if we ignore the change of the reconstruction, empirical potential calculations for Si/Si(100) indicate that the barriers change by ~0.1 eV for 2–3 % strain (compressive or tensile),[29] and more recent DFT calculations[13] for $In_xGa_{1-x}As(001)$ confirm a similar change of ~0.1 eV upon 4% (tensile) strain. These numbers correspond to a variation of D by approximately one order of magnitude at $T=700$ K.

The results discussed in this paper open the door to exploring new pathways for the self-organization of nano particles and quantum dots. Once one understands how artificial features (such as buried defects or dislocation lines) alter the PES, our results indicate if and how one can expect self-organization. We have shown that a properly modified PES can be exploited to obtain lateral ordering of islands. Both a modification of the transition energies, as well as a modification of the adsorption energies, can lead to self-organization. Thus, either the thermodynamics (modification of E_{ad}) as well as the kinetics (modification of E_{trans}) of the nucleation process can be used to influence and guide the self-assembly of patterns. Our results indicate that depending on the desired application, either modification might be more desirable: If one wants smaller islands, guided self-assembly in the thermodynamic limit might be more desirable, while guided self-assembly in the kinetic limit might be better suitable if one wants to obtain larger features.

It has been shown experimentally that buried defect lines or dislocations can indeed alter the spatial arrangement of islands.[10,11] Our simulations can explain such a guided arrangement of islands. Our simulations indicate that these patterns could be created by thermodynamic, as well as kinetic effects. Therefore, our results might in fact provide an alternative explanation to the study by Yang *et al.*,[15] where only the thermodynamics were offered as an explanation for guided self-assembly upon a strain mediated chemical potential.

The morphologies shown so far were all obtained at a

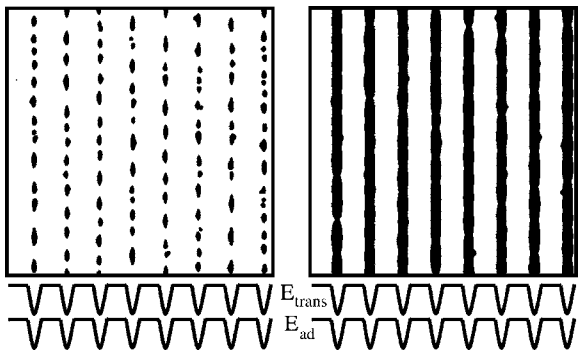

FIG. 4. Morphologies at coverages $\Theta=0.1$ ML (left) and $\Theta=0.3$ ML (right) obtained with a PES (below) that has a much narrower variation.

submonolayer precoalescence coverage of $\Theta=0.2$ ML and with a PES that varies sinusoidally. In Fig. 4 we show the morphology at different coverages obtained with PES that varies more sharply in certain regions, and is essentially constant in others. At $\Theta=0.1$ ML, the islands are aligned even better than in the previously discussed cases [in particular, cf. Fig. 3(b)]. Moreover, at $\Theta=0.3$ ML, all the islands that are aligned along the *j* direction have coalesced in this direction, while they do not touch at all along the *i* direction. In fact, we get a very regular array of one-dimensional, monolayer-high nanowires on the surface. Such wires can be used for a number of technological applications. One of the currently most promising techniques to produce such wires is electron-beam-induced deposition,[30] but there is a fundamental resolution limit for wires that are narrower than ~10 nm. Our simulations suggest a different mechanism for how such quantum wires can be obtained, with a width that can be much smaller.

The results in this Brief Report suggest an approach to guiding self-assembly of nano patterns. Application of this approach, even in simulation, will require several additional ingredients, including microscopic models of elasticity and of the strain dependence of the PES and other properties. Also, strain-induced changes of the PES due to the developing surface morphologies should be included in a more comprehensive model.[31] This is an ongoing challenge for computational material scientists. Nevertheless, our results indicate that interesting effects are to be expected, and our numerical approach makes it feasible to perform the (expensive) calculation of the elastic field at every timestep during the simulation.

This research was supported in part by the MARCO Center on Functional Engineered NanoArchitectonics (FENA) and by the NSF through Grant No. DMS-0402276.

*Corresponding author. Email address: cratsch@math.ucla.edu

[1] S. Sun, C. B. Murray, D. Weller, L. Folks, and A. Moser, Science **287**, 1989 (2000).
[2] M. Valden, X. Lai, and D. W. Goodman, Science **281**, 1647 (1998).
[3] For recent reviews, see V. A. Shchukin and D. Bimberg, Rev. Mod. Phys. **71**, 1125 (1999); J. Stangl, V. Holy, and G. Bauer, Rev. Mod. Phys. **76**, 725 (2004).
[4] D. J. Eaglesham and M. Cerullo, Phys. Rev. Lett. **64**, 1943 (1990).
[5] Y.-W. Mo *et al.*, Phys. Rev. Lett. **65**, 1020 (1990).
[6] S. Guha, A. Madhukar, and K. C. Rajkumar, Appl. Phys. Lett. **57**, 2110 (1990).
[7] C. Teichert *et al.*, Phys. Rev. B **53**, 16334 (1996).
[8] Q. Xie, A. Madhukar, P. Chen, and N. P. Kobayashi, Phys. Rev. Lett. **75**, 2542 (1995).
[9] B. Lita *et al.*, Appl. Phys. Lett. **74**, 2824 (1999).
[10] A. E. Romanov, P. M. Petroff, and J. S. Speck, Appl. Phys. Lett. **74**, 2280 (1999).
[11] H. J. Kim, Z. M. Zhao, and Y. H. Xie, Phys. Rev. B **68**, 205312 (2003).
[12] C. Ratsch, A. P. Seitsonen, and M. Scheffler, Phys. Rev. B **55**, 6750 (1997).
[13] E. Penev, P. Kratzer, and M. Scheffler, Phys. Rev. B **64**, 085401 (2001).
[14] J. Tersoff, C. Teichert, and M. G. Lagally, Phys. Rev. Lett. **76**, 1675 (1996).
[15] B. Yang, F. Liu, and M. G. Lagally, Phys. Rev. Lett. **92**, 025502 (2004).
[16] S. M. Wise *et al.*, Appl. Phys. Lett. **87**, 133102 (2005).
[17] C. Zhao *et al.*, J. Chem. Phys. **123**, 094708 (2005).
[18] T. R. Mattsson and H. Metiu, Appl. Phys. Lett. **75**, 926 (1999).
[19] R. F. Sabiryanov *et al.*, Phys. Rev. B **67**, 125412 (2003).
[20] M. Petersen *et al.*, Phys. Rev. E **64**, 061602 (2001).
[21] C. Ratsch *et al.*, Phys. Rev. B **65**, 195403 (2002).
[22] R. E. Caflisch *et al.*, Phys. Rev. E **59**, 6879 (1999).
[23] J. Venables, Philos. Mag. **27**, 697 (1973); G. S. Bales and D. C. Chrzan, Phys. Rev. B **50**, 6057 (1994).
[24] C. Wöll, S. Chiang, R. J. Wilson, and P. H. Lippel, Phys. Rev. B **39**, 7988 (1989).
[25] C. Ratsch *et al.*, Surf. Sci. **329**, L599 (1995).
[26] Strictly speaking, the hopping rate along the two opposite directions along the *i* axis is slightly different (by construction of the drift). But the average of these two rates is essentially constant along the *i* direction.
[27] H. Brune *et al.*, Phys. Rev. B **52**, R14380 (1995).
[28] C. Ratsch, Phys. Rev. B **63**, 161306(R) (2001).
[29] C. Roland and G. H. Gilmer, Phys. Rev. B **46**, 13428 (1992).
[30] N. Silvis-Cividjian *et al.*, Appl. Phys. Lett. **82**, 3514 (2003).
[31] M. T. Lung, C.-H. Lam, and L. M. Sander, Phys. Rev. Lett. **95**, 086102 (2005).